# Light diffuseness metric, Part 1

## Theory

Xia, Ling; Pont, Sylvia; Heynderickx, Ingrid

**DOI**
10.1177/1477153516631391

**Publication date**
2017

**Document Version**
Final published version

**Published in**
Lighting Research and Technology

*Lighting Res. Technol.* 2017; Vol. **49**: 411–427

# Light diffuseness metric Part 1: Theory

**L Xia** MSc[a], **SC Pont** PhD[a] and **I Heynderickx** PhD[b]
[a]Department of Industrial Design, $\pi$-lab (Perceptual Intelligence Laboratory), Delft University of Technology, Delft, The Netherlands
[b]Department of Human Technology Interaction, Eindhoven University of Technology, Eindhoven, The Netherlands

Received 15 September 2015; Revised 3 December 2015; Accepted 26 January 2016

The light density, direction and diffuseness are important indicators of the spatial and form-giving character of light. Mury presented a method to describe, measure and visualise the light field's structure in terms of light density and direction variations in three-dimensional spaces. We extend this work with a theoretical and empirical review of four diffuseness metrics leading to a novel metric proposal $D_{Xia}$. In particular, the relationships between these diffuseness metrics were studied using a model named 'probe in a sphere'. Diffuseness metric $D_{Xia}$ re-frames the diffuseness metric of Cuttle in an integral description of the light field. It fulfils all diffuseness criteria and has the advantage that it can be used in a global, integrated description of the light flow and diffuseness throughout three-dimensional spaces.

## 1. Introduction

Since the lighting profession emerged, lighting standards around the world have been concerned almost exclusively with the delivery of luminous flux onto planes.[1] However, it is the distribution of light that determines the appearance of a space and the objects inside it. Inspiringly, this concept has been well acknowledged by photographers,[2] painters,[3,4] designers[5] and architects,[6,7] Rather than thinking about the illumination as a medium that makes things visible, modern designers prefer to see lighting principally in terms of how it influences the appearance of people's surroundings and creates certain atmospheres.[8–13]

In their psychophysical research, Koenderink *et al.*[14] found that human observers have expectations of what an object would look like when it was introduced at an arbitrary location in a scene. Schirillo[15] confirmed that human observers have a mental representation of the light in a three-dimensional space through both direct and indirect evidence of our awareness of the light field. The light field in natural scenes is highly complicated due to intricate optical interactions, containing low and high frequencies in the radiance distribution function. Nonetheless, studies show that the human visual system is able to distinguish the intensity, the primary illumination direction, and the diffuseness, which are three basic (low-order) properties of a light field.[14,16–18] Furthermore, research showed that these low order properties of the light field stay rather constant within a certain geometry of the scene[19] and that they are sufficient to describe the appearance of most natural materials because the diffuse scattering characteristic of these materials acts as a low pass filter.[20–23]

By introducing the notion of radiant 'light density' and the notion of 'light vector', Gershun[24] described the quantity and transfer direction of the radiant power through space in his 5-dimensional function of the light field. Mury[25] used spherical harmonic (SH)

Address for correspondence: Ling Xia, Department of Industrial Design, $\pi$-lab (Perceptual Intelligence Laboratory), Delft University of Technology, Landbergstraat 15, 2628 CE Delft, The Netherlands.
E-mail: L.Xia-1@tudelft.nl


10.1177/1477153516631391

decompositions to represent natural light as a combination of components of different orders. He found that the zeroth order component of the SH decomposition corresponds to Gershun's 'density of light', which describes a constant illumination from all directions and is usually known as 'ambient light' in computer graphics; the first order component was found to correspond to the 'light vector' as defined by Gershun, which describes the net transport of radiant energy. However, neither Gershun nor Mury mentioned diffuseness of light in their mathematical descriptions of the physical light field.

The local light diffuseness describes the isotropy of a light distribution around a point in a space. It ranges from fully collimated light via hemispherical diffuseness to completely diffuse light. Fully collimated light comes from a single direction; in contrast, completely diffuse light comes from a sphere of directions. Light diffuseness can strongly influence the appearance of scenes and objects in it, because shading, shadowing and vignetting effects co-vary with the diffuseness, as can be seen in Figure 1. Direct sunlight is a typical example of collimated light, an overcast sky of hemispherical diffuse light and a polar whiteout of completely diffuse light. Collimated light creates an effect of focusing by generating hard, crisp-edged body shadows and a large brightness contrast, like the visual effect on sculptures in a museum created by spotlights. Hemispherical diffuse light is the level of diffuseness that we encounter in daily life most frequently, for instance under a cloudy sky. Completely diffuse light is characterised by a totally uniform light distribution and makes three-dimensional shapes appear flat, e.g. as the scenery when skiing in the mist.

The influence of the spatial distribution of light on object shape appearance has been studied through the notion of 'modelling index' in interior lighting design. Examples are the 'ratio between the cylindrical and horizontal illuminance' by Hewitt *et al.*,[26] the 'vector/scalar illumination ratio' (i.e. the strength of flow of light) by Cuttle,[27,28] and the vertical and horizontal modelling indicators (VMI and HMI) by Bean.[29] Since these 'modelling indices' are highly correlated with the light diffuseness, they are also considered as diffuseness metrics in our study. But, apart from using these 'modelling indices', we focus in the rest of this study on the light distribution, and not its effects on object appearance or how the resulting optical structures are interpreted by the human visual system. Relationships between the light diffuseness and objects' appearance are addressed in detail in other studies.[6,30–32]

Besides the 'modelling indices', other practical ways to quantify diffuseness have been proposed. Frandsen proposed the scale of light to indicate the potential of an illumination distribution to form shadow patterns over 3D opaque objects.[33] Morgenstern *et al.*[31,34] proposed the ICE (Illuminance Contrast Energy), a measure of the contrast over a white matte spherical gauge object. Inanici[35] used the directional-to-diffuse ratio to quantify the diffuseness of light by isolating the diffuse and directional components of a rendered luminous environment.

Thus, various practically defined diffuseness metrics exist but they differ from each other by definition and have been implemented in different fields. In order to propose a general and principled way to define and measure light diffuseness, we defined criteria for the diffuseness metric: A. The metric should describe the full range of diffuseness in a smooth and monotonic manner, B. It should be possible to physically measure the metric, C. The metric should describe the light distribution directly instead of via the appearance of some object, D. It should be possible to easily implement the metric in commercially available optical measurement systems as well as in computer simulations and in a manner that relates to human perception.

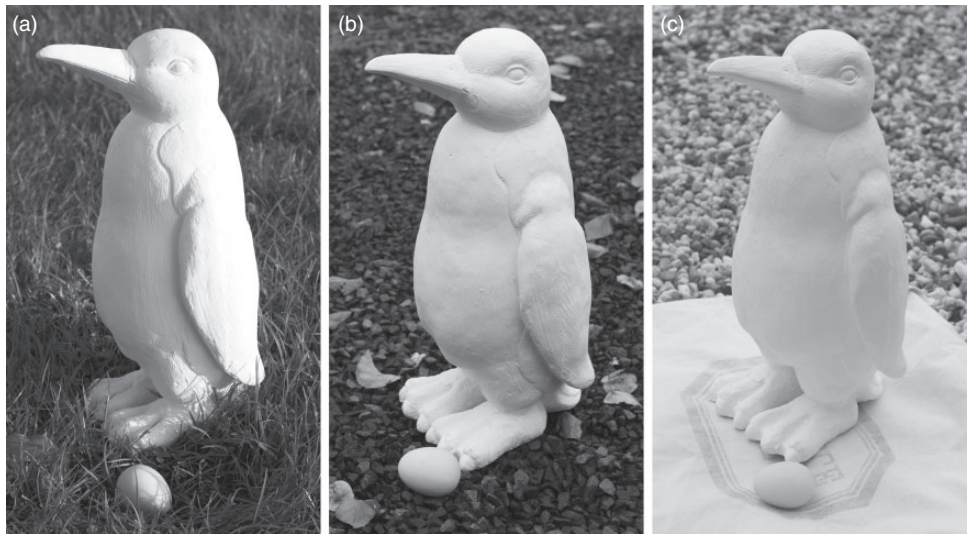


**Figure 1.** The appearance of a penguin statue under light with different diffuseness levels: (a) direct sunlight, (b) overcast sky above a dark ground surface, and (c) overcast sky above a light ground surface.

In the following sections, we give a review of four well-known diffuseness metrics, which are (1) the 'scale of light' by Frandsen,[33] (2) the 'ratio between cylindrical and horizontal illuminance' by Hewitt *et al.*,[26] (3) the 'ratio between illumination vector and scalar' by Cuttle,[27,28] and (4) the 'ICE' by Morgenstern *et al.*[31] We compare each of these four metrics to the criteria proposed above. Next, inspired by Mury's work on the physical SH representation of the light field and by the basic parameterisation of diffuseness as the balance between the ambient and directed light, we prove that Cuttle's 'ratio between illumination vector and scalar' (hereafter referred to as $D_{Cuttle}$) is equivalent to the ratio between the strength of the first order (i.e. the light vector) and the zeroth order (i.e. the light density) of the SH representation of the light field (this ratio is hereafter referred to as $D_{Xia}$. The diffuseness metric $D_{Xia}$ is entirely based on a mathematical description of the physical light distribution and fulfils all the criteria mentioned above.

Since the relationships between these metrics were so far unclear, we examined them via a model named 'probe in a sphere'. As Figure 2 illustrates, this model consists of a probe (usually, a small white sphere with a Lambertian surface) put right in the centre of a big spherical light source with a variable subtended angle. The size of the functional light source is defined by the subtended angle $\alpha$ (see the upper arc depicting the spherical light source in Figure 2). The diameter of the spherical light source is much larger than the probe inside (i.e. which basically means that it is at infinity). Thus, by varying the subtended angle $\alpha$ from $0^\circ$ via $180^\circ$ to $360^\circ$, the degree of diffuseness varies from totally collimated light via hemispherical diffuse to completely diffuse light. This model was first implemented by Cuttle to investigate how the surrounding luminous field influenced the vector/scalar ratio.[6] The model 'probe in a sphere' should be considered as a physics model (a simplified representation of something that is either too difficult or impossible to display directly) for natural situations (like daylight on a city square, museum lighting and office lighting). It allows systematic theoretical studies and comparisons of metrics. In addition, in our

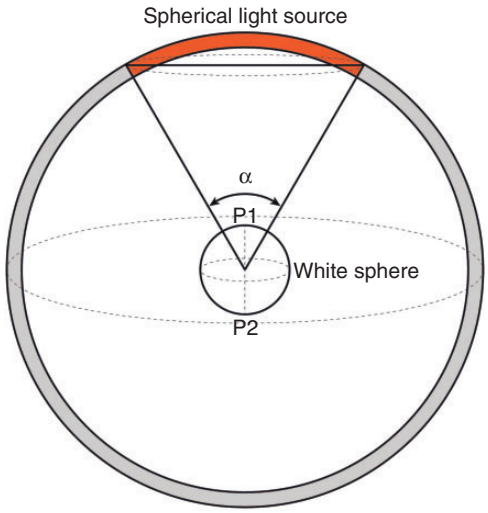


**Figure 2.** Illustration of the computational model 'probe in a sphere', a white Lambertian sphere is put right in the centre of a large spherical light source. The size of the light source varies with the subtended angle $\alpha$. The outer spherical light source is assumed to be at infinity.

second paper 'Light diffuseness metric Part 2' we consider empirically measured light fields.

## 2. Frandsen's scale of light

### 2.1. Theory

Frandsen proposed the scale of light, which is derived from the comparison between the size of a light source and that of an illuminated object. This relationship is reflected by the self-shadows on an object, which indicate the degree of light diffuseness.[33] Yağmur and Ozturk recently found that the harshness-softness attribute of cast-shadows also depends on the scale of light; the shadows are softer when the luminaire size increases, or the object size decreases.[36]

Frandsen's approach is analogous to our 'probe in a sphere' approach. In Frandsen's theory, the solid angle of light source ($\alpha$ in our model) varied from narrow (i.e. 0°, collimated) to hemispherically diffuse (i.e. 180°). As Figure 3(a) shows, when the subtended angle is smaller than 180°, the white sphere can be divided into three zones. The top zone facing the circular light source receives light from the entire source. The bottom zone turned away from the source receives no light. The middle zone receives a varying amount of light from the source, creating a so-called semi-shadow. Frandsen scaled the diffuseness in the range from fully collimated to hemispherical diffuseness based on the ratio of the area of the semi-shadow to the area of the whole sphere. Diffuseness then increases from 0% to 100%, as the subtended angle varies from 0° to 180°. Frandsen scaled this change into 11 steps with an interval of 10%. The left part of Table 1 gives detailed information about the scale of light from a fully collimated light to a hemispherical diffuse light as defined by Frandsen ($D_{Frandsen}$).

The scale of light, however, is hard to measure in a real environment. It cannot be judged accurately from the appearance of objects, for instance using a matte sphere as a reference, because small steps in diffuseness are hard to be distinguished in this manner.[18,37–39] Moreover, perceived diffuseness is dependent on viewing direction.[18,40] Furthermore, Frandsen's scale with 11 types of shadows is limited to the range from fully collimated light to hemispherical diffuse light. The other half ranging from hemispherical diffuse to completely diffuse light is ignored. So, the scale of light does not fulfil criteria A, B, C and D.

### 2.2. $D_{Frandsen}$ for the 'probe in a sphere' model

In order to be able to compare all metrics, we extended $D_{Frandsen}$ to the full range of possible diffuseness. As Figure 3(b) shows, when the subtended angle is larger than 180°, the white sphere can be divided into two zones. The top zone always receives the same amount of light, as it would from a hemispherical light source. The middle zone receives a varying amount of light from the source. The bottom zone disappears because

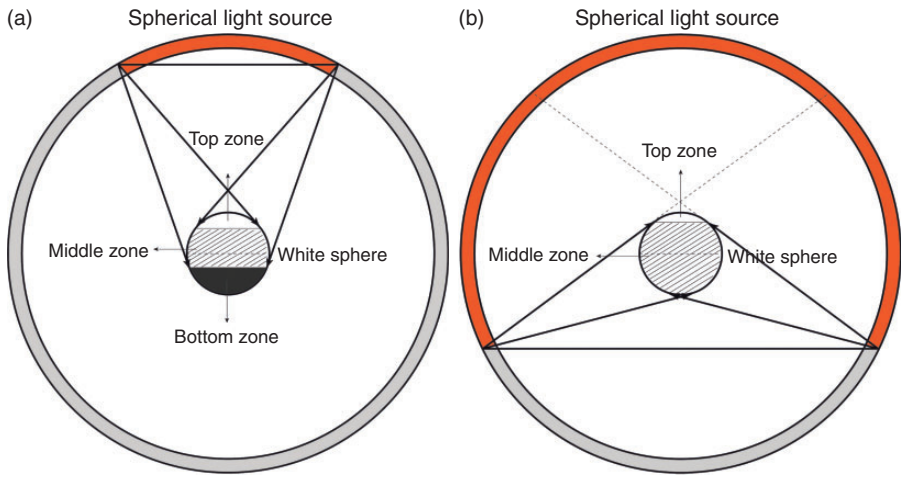


**Figure 3.** Illustration of shadowing zones on a white matte sphere according to Frandsen. In (a): when the subtended angle is smaller than 180°, the white sphere in the centre of the spherical light source is divided into three zones: the top zone receives light from the entire source, the middle zone receives a varying amount of light from the source, and the bottom zone receives no light from the source. In (b): when the subtended angle is larger than 180°, the white sphere in the centre of the spherical light source is divided into two zones: there's no bottom zone receiving no light.

**Table 1.** The left part shows the scale of light as defined by Frandsen, for the range of collimated light to hemispherical diffuse light; the right part shows our extension of the scale of light, for the range from hemispherical diffuse to totally diffuse light.

| $D_{Frandsen}$ | | | Extended $D_{Frandsen}$ | | |
|---|---|---|---|---|---|
| $\alpha$ | Ratio, % | Scale | $\alpha$ | Ratio, % | Scale |
| $\approx 0°$ | 0 | 0 | 231.7° | 95 | 11 |
| 11.5° | 10 | 1 | 253.7° | 90 | 12 |
| 23.1° | 20 | 2 | 271.1° | 85 | 13 |
| 34.9° | 30 | 3 | 286.2° | 80 | 14 |
| 47.1° | 40 | 4 | 300° | 75 | 15 |
| 60.0° | 50 | 5 | 312.8° | 70 | 16 |
| 73.7° | 60 | 6 | 325.1° | 65 | 17 |
| 88.9° | 70 | 7 | 336.9° | 60 | 18 |
| 106.3° | 80 | 8 | 348.5° | 55 | 19 |
| 128.3° | 90 | 9 | 360° | 50 | 20 |
| 180° | 100 | 10 | | | |

every part of the sphere is now illuminated. As a consequence, we can extend the scale of light from hemispherical diffuse to totally diffuse by still using the ratio of the area of the semi-shadow to the area of the whole sphere as proposed by Frandsen. As the subtended angle gets larger, the area of the top zone increases and the ratio of the semi-shadow to the area of the whole sphere decreases, but this ratio always remains larger than 50%. We used an interval of 5% in the ratio in order to divide the scale in an equal number of steps for the extended part of the range as for the original range from collimated to hemispherical diffuse. In this manner, we extended Frandsen's scale of light from 0–10 to 0–20. The right part of Table 1 gives detailed information about this extended scale, and the appearance of a Lambertian white sphere under the different scale values is illustrated in Figure 4. The resulting values are shown in Figure 7(a) and (b).

## 3. Hewitt *et al.*'s cylindrical/horizontal illuminance ratio

### 3.1. Theory

People have noticed that compared to horizontal illumination, which is a provision

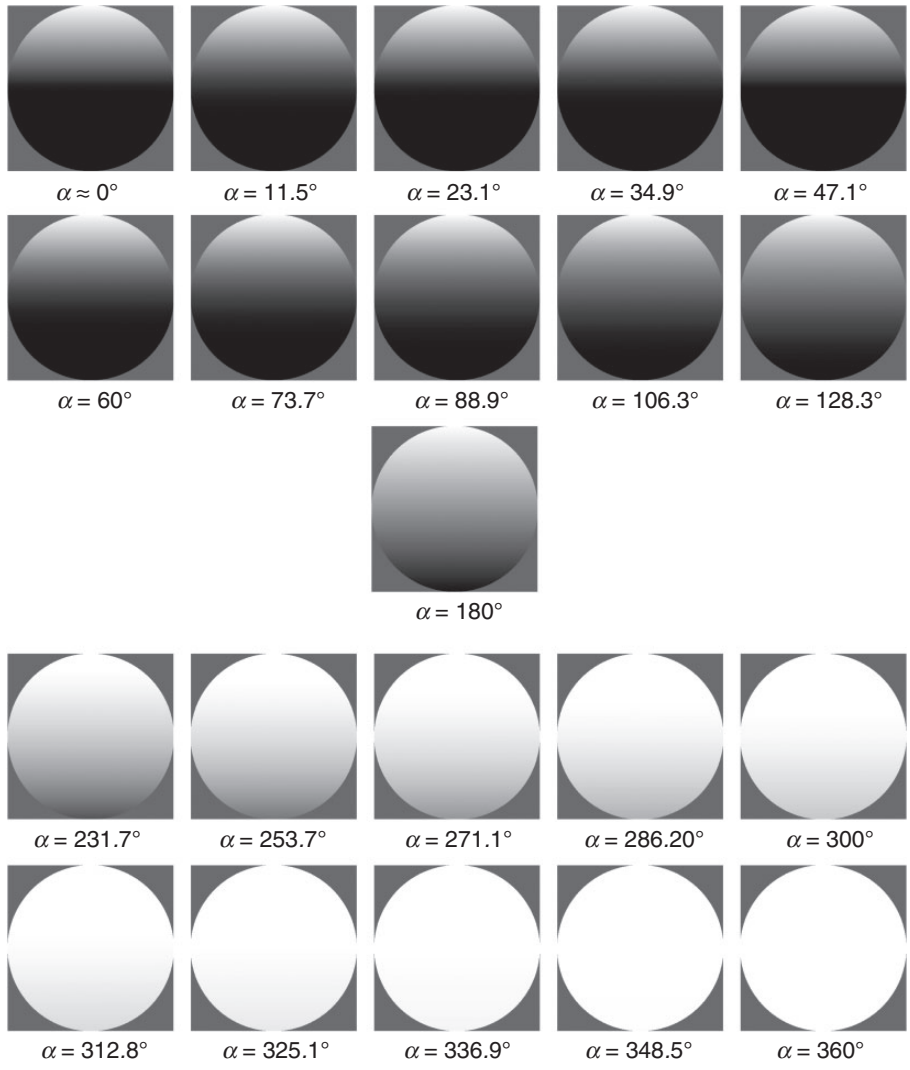


**Figure 4.** The appearance of a rendered Lambertian white sphere in the centre of a large spherical light source with variable subtended angle $\alpha$. The subtended angle varies from 0° via 180° to 360°, and the corresponding diffuseness varied from fully collimated light via hemispherical diffuse to totally diffuse light.

of task illumination, vertical illumination contributes more to the impression of a space and helps people to recognise shapes and faces. Hewitt *et al*. have shown that the ratio of horizontal illuminance to mean vertical illuminance gives a reasonable indication of modelling.[26] The average vertical illuminance can be measured using the cylindrical illuminance, which is defined as the total luminous flux falling on the curved surface of a small cylinder at a point of interest, divided by the curved surface area of the cylinder.[41] Instruments exist for the direct measurement of cylindrical illumination, but their costs are high. An alternative method for obtaining cylindrical illuminance was proposed by Duff

*et al.*, i.e. calculating it from the illuminance values measured using a cubic illumination meter.[42,43] The ratio between the cylindrical illuminance ($E_C$) and horizontal illuminance ($E_h$) is proposed as an index of modelling for overhead lighting installations[1] and is hereafter referred to as diffuseness metric $D_{Hewitt}$. A modelling index between 0.3 and 0.6 is suggested to indicate good modelling.[1]

The ratio between cylindrical and horizontal illuminance does fulfil the criteria we have defined for a diffuseness metric. However, it can only indicate the 'modelling' properties of an overhead lighting installation. For pure overhead lighting it is assumed to provide a rough assessment of the relationship between the rather diffuse light from (inter-reflections) and the rather directed light from primary light sources. However, the assumptions are violated in many real scenes, for instance if there is also light entering from the side via windows.

### 3.2. $D_{Hewitt}$ for the 'probe in a sphere' model

We calculated $D_{Hewitt}$ in the 'probe in a sphere' model by replacing the white sphere with a small cylinder. The cylinder was placed with its main axis along the vertical axis in Figure 2 so that the average illuminance on the curved surface represents the mean vertical illuminance. $D_{Hewitt}$ varied from '0' for collimated light to '1' for fully diffuse light. The resulting values as a function of subtended angle $\alpha$ are shown in Figure 7(a) and (b).

## 4. Cuttle's vector/scalar illumination ratio

### 4.1. Theory

Hewitt[44] and Lynes *et al.*[28] proposed the concept of the 'flow of light' to describe the potential of light to produce distinct shading patterns. The 'flow of light' concept gives information on the direction from which the light comes on average, and on how strongly directed the net light transport is. Cuttle *et al.*[44] defined the apparent strength of the 'flow of light' by the illumination vector/scalar ratio ($E_{vector}/E_{scalar}$), and recommended it as a modelling index . We refer to $E_{vector}/E_{scalar}$ as diffuseness metric $D_{Cuttle}$. The vector component indicates the direction of the 'flow of light'. The illumination scalar equals the average value of the 'illumination solid' over all directions, and it is a measure of the ambient light. In general, the 'illumination solid' around an illuminated point can be separated into two components: a vector component and a symmetric component. The vector component is totally asymmetric around the illuminated point, while the symmetric component is totally symmetric around the illuminated point.[6,27]

Though the illumination vector and scalar are defined based on the luminous density distribution in the space, their values and the metric are explained via the appearance of a small matte white sphere. The illumination vector can be reproduced by a distant light source with the illuminance falling on a small sphere as illustrated in Figure 5. The magnitude of the vector illuminance can then be approached as the difference between the illuminance on the top point and the bottom point of the matte white sphere:

$$E_{vector} = E_{p1} - E_{P2} \tag{1}$$

The scalar illuminance value equals the average illuminance over the whole surface of the sphere and can be calculated as

$$E_{scalar} = \frac{E_{vector}}{4} + \bar{E}_{symmetric} \tag{2}$$

where $\bar{E}_{symmetric}$ is the average value of the symmetric component over all directions. Thus, the maximum value of $D_{Cuttle}$ is 4, occurring with fully collimated light (i.e. the vector component only) and the minimum value is 0, occurring with completely diffuse

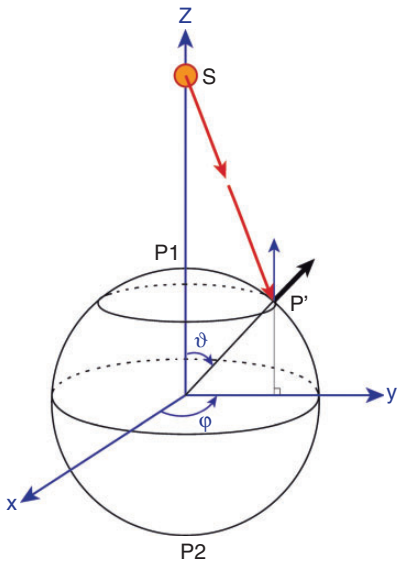


**Figure 5.** Illustration of a unit matte sphere in Figure 2 under a fully collimated light with the subtended angle $\alpha$ approaching 0°. P1 is the top point of the white sphere and P2 is the bottom point of the white sphere.

light (i.e. the symmetric component only). It has been found that $D_{Cuttle}$ values in the range of 1.2 to 1.8 are preferred for the appearance of human features in an interview situation.[44] Preference studies also showed that people like the flow of light to be from the top-left/right rather than from the top, with a preference for a vector altitude between 15° and 45°.[44]

Later, Cuttle developed a cubic illumination meter to measure the illumination vector, the illumination scalar and the strength of the 'flow of light' or $D_{Cuttle}$.[45,46] The cubic illumination meter is a small cube with six illuminance meters mounted at its six faces. Thus, Cuttle's method fulfils all our criteria for a diffuseness metric.

### 4.2. $D_{Cuttle}$ for the 'probe in a sphere' model

The illumination scalar proposed by Cuttle in equation (2) represents the average illumination over the sphere surface, derived from the contributions of both the vector and the symmetrical components. The vector component contributes $E_{vector}/4$ to the average illumination over the matte sphere, which can be derived analytically. For instance in Figure 5, the bottom hemisphere receives no light ($E_{p2} = 0$) and the illumination falling on the upper hemisphere is directly proportional to the cosine of the angle $\vartheta$ between the direction of the light source (i.e. the z axis) and the surface normal. So, the contribution of the vector component to the average illumination over the unit sphere follows:

$$\begin{aligned}(E_{vector})_{scalar} &= (E_{p1} - E_{p2})\frac{\int_0^{2\pi}\int_0^{\frac{\pi}{2}}\cos(\vartheta)\sin(\vartheta)\mathrm{d}\vartheta\mathrm{d}\varphi}{4\pi} \\ &= (E_{p1} - E_{p2})/4 \\ &= E_{vector}/4 \end{aligned} \quad (3)$$

By varying the subtended angle from 0° to 360°, the diffuseness level in our model 'probe in a sphere' varies from fully collimated light to fully diffuse light while the vector/scalar illumination ratio varies from 4 to 0 as shown in Figure 7(a). The normalised form of $D_{Cuttle}$ is

$$(D_{Cuttle})_{Normalized} = 1 - (E_{vector}/E_{scalar})/4 \quad (4)$$

which is shown in Figure 7(b), with '0' corresponding to fully collimated light and '1' corresponding to fully diffuse light.

## 5. Morgenstern *et al.*'s illuminance contrast energy

### 5.1. Theory

The contrast of a shading pattern over a sphere varies with the degree of light diffuseness. Morgenstern *et al.* defined a new method, the ICE (Illuminance Contrast Energy) to quantify this variation.[31] If $E(\vartheta, \varphi)$ is the illuminance over the surface of a unit sphere, where $\vartheta$ is the altitude from the north pole and

$\varphi$ is the azimuth in a spherical coordinate system, the ICE can be calculated as:

$$ICE = \left( \frac{1}{4\pi} \int_0^{2\pi} \int_0^{\pi} \left( \frac{E(\vartheta,\varphi) - \bar{E}}{\bar{E}} \right)^2 \times \sin(\vartheta) \mathrm{d}\vartheta \mathrm{d}\varphi \right)^{1/2} \quad (5)$$

where $\bar{E}$ is the mean illuminance over the sphere. The value of ICE ranges from 0 for a completely diffuse light to 1.29 for a distant point light source. In order to measure the ICE, Morgenstern *et al.* used a custom-built multi-directional photometer with 64 evenly spaced photodiodes. These 64 photodiodes made low-resolution but omnidirectional records of the illumination incident from all directions at a point in space at a given time. As such, ICE does not fulfil criterion D, because it cannot be measured in real scenes without the custom-built photometer. It does not literally fulfil criterion C because in order to calculate the ICE the photometer records have to be transformed to values of the illuminance over the gauge sphere. Using their photodiode device, Morgenstern *et al.* made 570 measurements of the ICE in six natural environments and 53 measurements in a single day from sunrise to sunset.[31] The mean ICE under these circumstances ranged from 0.41 to 0.66.

### 5.2. $D_{Morgenstern}$ for the 'probe in a sphere' model

We calculated the ICE directly from the illuminance distribution on the small white Lambertian sphere inside the spherical model using equation (5). The resulting values as a function of subtended angle $\alpha$ are shown in Figure 7(a) and (b). The resulting curve is less than 6% higher than the $D_{Cuttle}$ curve in the lower and middle part of the diffuseness range. Overall, the shape of the curve $D_{Morgenstern}$ in this model clearly closely resembles the shape of the $D_{Hewitt}$ and $D_{Cuttle}$ curves.

## 6. $D_{Xia}$: framing 'diffuseness' in an integral light field description

From the above review we found that $D_{Morgenstern}$ and $D_{Frandsen}$ did not fulfil all criteria for a diffuseness metric. $D_{Hewitt}$ fulfilled all criteria, but was limited to indicate the light diffuseness properties of overhead lighting. $D_{Cuttle}$ fulfilled all criteria. However, the relationship between $D_{Cuttle}$ and the other properties of the light field (i.e. light density, direction) has not been worked out. In this section, we therefore frame this diffuseness definition in an integral light field description. We call the framed metric $D_{Xia}$, which is thus conceptually the same as $D_{Cuttle}$ but mathematically framed in a different way. The description of $D_{Xia}$ is based on a mathematical description of the physical light distribution in space instead of on the appearance of an object. $D_{Xia}$ fulfils all criteria and has the advantage that it can be used in a global, integrated description of the light distribution in 3D spaces, in which all modes of the description have a specific physical meaning. The development of $D_{Xia}$ is based on the work of Mury *et al.*,[19,47,48] i.e. on the physical interpretation of the spherical harmonics representation of the light field in natural scenes, and extends it with a diffuseness metric.

### 6.1. Theory

Locally, the light field is a function of direction and thus a spherical function. We know that any spherical function $f(\vartheta,\varphi)$ can be reconstructed by the sum of its spherical harmonics (SH)

$$f(\vartheta,\varphi) = \sum_{l=0}^{\infty} \sum_{m=-l}^{l} C_l^m Y_l^m(\vartheta,\varphi) \quad (6)$$

where $C_l^m$ are the coefficients, $Y_l^m(\vartheta,\varphi)$ are the basis functions, and $l$ represents the order of the angular mode. Each mode consists of $2l+1$ basis functions $(l \geq 0, -l \leq m \leq l)$. Figure 6 shows the real-valued spherical

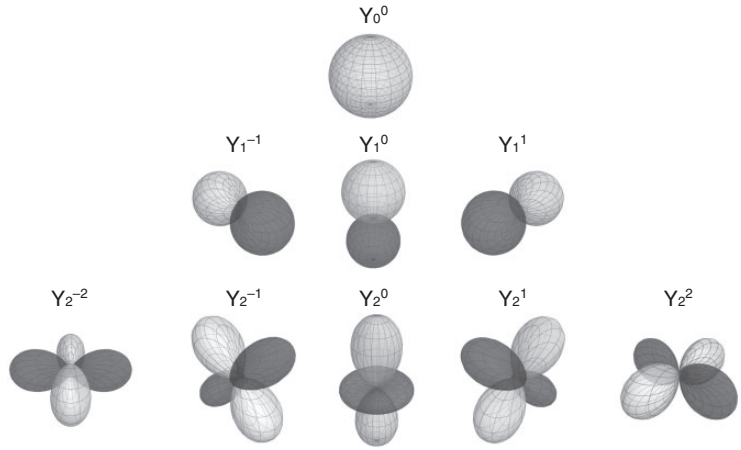


**Figure 6.** Plots of real-valued spherical harmonic basis functions. The first row represents the zeroth order, the second row shows the basis functions of the first order and the third row shows the basis functions of the second order components. Light grey indicates positive values and dark grey indicates negative values. For a detailed explanation of the analogy between the SH description and Gershun's theory, see work by Mury *et al.*[19,25,47]

harmonic basis functions up to the second order. Any mode $l$ can be represented as a vector of corresponding coefficients $SH_l(f) = \left\{ C_l^{-l},\ C_l^{-l+1},\ \cdots, C_l^{l} \right\}$ and the representation of the entire function is a combination of all the modes, i.e. $SH(f) = \left\{ SH_0(f),\ SH_1(f),\ SH_2(f),\ \cdots \right\}$. The strength of each mode $l$ can be calculated using equation (7)[49]

$$d(SH_l) = \sqrt{\sum_{m=-l}^{l} (C_l^m)^2} \tag{7}$$

Ramamoorthi and Hanrahan proved that for convex Lambertian objects, complex lighting distributions may be successfully replaced by the second order approximation of their SH representation.[23] Mury *et al.*[19,25,47] found that the zeroth order component of a spherical harmonic corresponds to Gershun's 'density of light'. The zeroth order component is a monopole (see the first row of Figure 6), essentially the average radiance over all directions. The first order component corresponds to Gershun's 'light vector' and describes the net transport direction of radiant energy. The first order component can be thought of as a dipole and consists of a positive and a negative mode (see the second row of Figure 6). We define our diffuseness metric as the ratio between the light vector and the density of light, or in mathematical SH terms

$$D_{Xia} = d(L_1)/d(L_0) \tag{8}$$

$D_{Cuttle}$ and $D_{Xia}$ are thus conceptually the same, but mathematically they are framed in a different manner. So, how are they mathematically related to each other and what are the (dis)advantages of the two approaches? In order to answer this question, we first express $D_{Xia}$ in terms of the ratio $d(E_1)/d(E_0)$ which is the ratio between the first order and zeroth order SH modes of the irradiance. Ramamoorthi and Hanrahan[23] proved that for convex Lambertian objects, the relation between irradiance and radiance of the zeroth order SH coefficient is

$$E_0^0 = \pi \times L_0^0 \tag{9}$$

and of the first order SH is

$$E_1^m = \frac{2\pi}{3} \times L_1^m, \qquad m = -1, 0, 1 \tag{10}$$

Hence

$$\frac{d(L_1)}{d(L_0)} = \frac{3}{2}\frac{d(E_1)}{d(E_0)} \tag{11}$$

Second, we express $D_{Cuttle}$ defined as the ratio between $E_{vector}$ and $E_{scalar}$, in terms of $d(E_1)/d(E_0)$. To do so, we first examine the relationship between $d(E_1)$ and $E_{vector}$. $E_{vector}$ was defined as the maximum value of the illuminance difference. However, the SH representation of the illumination distribution accounts for the illumination in all directions. Therefore, we calculated the magnitude of the vector component over the surface of a sphere projected along the direction of the light vector (e.g. the z axis in Figure 5) as:

$$E'_{vector} = (E_{p1} - E_{p2}) \times \int_0^{2\pi} \int_0^{\frac{\pi}{2}} \cos(\vartheta)\cos(\vartheta) \sin(\vartheta)\mathrm{d}\vartheta\mathrm{d}\varphi = \frac{2\pi}{3}(E_{p1} - E_{p2}) \tag{12}$$

Thus, the magnitude of the vector component over the surface of a sphere $E'_{vector}$ is a factor of $2\pi/3$ larger than Cuttle's $E_{vector}$.

The first order component of the SH approximation of the light field can be transformed into linear functions of the Cartesian coordinates (x, y, z) as follows

$$\begin{cases} Y_1^{-1}(\vartheta,\varphi) = -\sqrt{\frac{3}{4\pi}}\sin\vartheta\sin\varphi = -\sqrt{\frac{3}{4\pi}}y \\ Y_1^{0}(\vartheta,\varphi) = \sqrt{\frac{3}{4\pi}}\cos\vartheta = \sqrt{\frac{3}{4\pi}}z \\ Y_1^{1}(\vartheta,\varphi) = -\sqrt{\frac{3}{4\pi}}\sin\vartheta\cos\varphi = -\sqrt{\frac{3}{4\pi}}x \end{cases} \tag{13}$$

According to equations (12) and (13), the relationship between the magnitude of the light vector $E_{vector}$ and the magnitude of the first order SH component $d(E_1)$ is

$$E_{vector} = \frac{3}{2\pi}E'_{vector} = \frac{3}{2\pi}\sqrt{\frac{4\pi}{3}}d(E_1) = \sqrt{\frac{3}{\pi}}d(E_1) \tag{14}$$

Subsequently, the relationship between $d(E_0)$ and $E_{scalar}$ *i*s derived. The illumination scalar is the average illuminance over the surface of a unit sphere, so $E_{scalar} = E_O/4\pi$, where $E_O$ is the overall illumination on the sphere. We find

$$\begin{aligned} \frac{E_{scalar}}{\mathrm{d}(E_0)} &= \frac{E_O/4\pi}{C_0^0} \\ &= \frac{1}{4\pi}\frac{\int_{\varphi=0}^{2\pi}\int_{\vartheta=0}^{\pi} f(\vartheta,\varphi)\sin\vartheta\mathrm{d}\vartheta\mathrm{d}\varphi}{\int_{\varphi=0}^{2\pi}\int_{\vartheta=0}^{\pi} f(\vartheta,\varphi)\,Y_0^0(\vartheta,\varphi)\sin\vartheta\mathrm{d}\vartheta\mathrm{d}\varphi} \\ &= \frac{1}{2\sqrt{\pi}} \end{aligned} \tag{15}$$

Knowing all this, we find the relationship between $d(L_1)/d(L_0)$ (or $D_{Xia}$) and $E_{vector}/E_{scalar}$ (or $D_{Cuttle}$) as

$$\begin{aligned} \frac{E_{vector}}{E_{scalar}} &= \frac{\sqrt{3/\pi}}{1/2\sqrt{\pi}}\frac{d(E_1)}{d(E_0)} = 2\sqrt{3}\frac{2}{3}\frac{d(L_1)}{d(L_0)} \\ &= \frac{4}{\sqrt{3}}\frac{d(L_1)}{d(L_0)} \end{aligned} \tag{16}$$

Hence, the ratio between the illumination vector and scalar is a factor $2\sqrt{3}$ larger than $d(E_1)/d(E_0)$ and $4/\sqrt{3}$ larger than $d(L_1)/d(L_0)$. This result indicates that the diffuseness metric vector/scalar illumination ratio ($D_{Cuttle}$) is equivalent to the ratio between the strength of the first order and zeroth order of the SH representation of the physical light distribution (i.e. $D_{Xia}$). The only difference is that $D_{Cuttle}$ is derived from the illuminance and $D_{Xia}$ from the luminance. Since the ratio between $E_{vector}$ and $E_{scalar}$

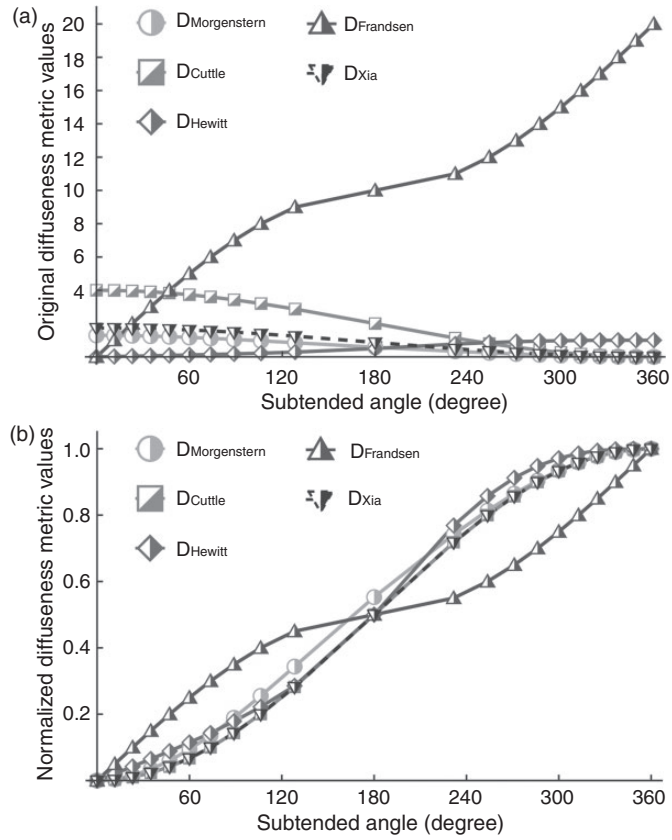


**Figure 7.** The five diffuseness metrics as a function of the subtended angle $\alpha$ in the model 'probe in a sphere': (extended) $D_{Frandsen}$, $D_{Hewitt}$, $D_{Cuttle}$, $D_{Morgenstern}$ and $D_{Xia}$. In (a) the original metric values and in (b) all diffuseness metrics normalised to the range (0–1) with '0' corresponding to fully collimated light and '1' corresponding to fully diffuse light.

varies from 4 for fully collimated light to 0 for fully diffuse light, we normalised the metric to a range 0 to 1. The final normalised form of $D_{Xia}$ is

$$(D_{Xia})_{Normalized} = 1 - d(L_1)/d(L_0)/\sqrt{3} \quad (17)$$

The diffuseness metric $D_{Xia}$ fulfils all the criteria we proposed before, and it is easily quantified and physically described based on a mathematical representation of the light field in 3D spaces.

### 6.2. $D_{Xia}$ for the 'probe in a sphere' model

We fitted SH representations to the luminance maps of our model, varying the subtended angle $\alpha$ from 0° to 360°. Then, the strength of the first and zeroth order components as well as their ratio ($d(L_1)/d(L_0)$) were calculated, and the results of $D_{Xia}$ are shown in Figure 7(a). The normalised curves of $D_{Cuttle}$ and $D_{Xia}$ in Figure 7(b) indeed overlap.

## 7. Results and discussion

Figure 7(a) illustrates the relationships between the five different diffuseness metrics

mentioned above. To get a better overview of these relationships, we normalised all diffuseness metrics with '0' corresponding to fully collimated light and '1' corresponding to fully diffuse light in Figure 7(b). In Figure 7(b) we see that the normalised diffuseness metrics $D_{Hewitt}$, $D_{Cuttle}$, $D_{Morgenstern}$ and $D_{Xia}$ give very similar results for the 'probe in a sphere' model. However, there is a difference between these normalised diffuseness metrics and $D_{Frandsen}$. It should be noticed that while the other diffuseness metrics concern ratios, the 'scale of light' ($D_{Frandsen}$) is an ordinal ranking. Since we want the metric to be perceptually relevant we need psychophysical data to make an arguable choice for the best metric. We are not aware of literature that relates perceptual diffuseness ratings to systematic variations of the physical diffuseness. We are only aware of perceptual matching data for diffuseness.[14,18,37–39] However, since the ratio-based metrics result in curves that resemble typical psychometric curves, we assume that these present the most plausible options for a perceptually relevant metric.

Morgenstern *et al.* made 570 measurements of the ICE in natural environments.[31] The results showed that the mean ICE ranged from 0.41 to 0.66 in these environments, which after normalisation means a range from 0.5 to 0.7. Cuttle *et al.* found a preference for the $E_{vector}/E_{scalar}$ ratio in the range from 1.2 to 1.8 for the appearance of human features in an interview situation.[44] This range corresponds to values between 0.55 and 0.7 for the normalised $D_{Cuttle}$. Thus, this range coincides with the diffuseness levels of natural scenes that Morgenstern found and indicates that human features presented in lighting environments with natural diffuseness levels are most preferred by human observers. A $D_{Hewitt}$ index in the range from 0.3 to 0.6 was noted to indicate good modelling.[1] The latter range corresponds to a normalised range from 0.3 to 0.6, and so partly overlaps with natural diffuseness levels, but also is partly extended towards more directed light. The latter guideline for the modelling index, however, was based on tests using statues of faces instead of real faces. It is probable that for statue illumination or museum lighting the light is preferred to be a bit more directed than natural light. Regarding $D_{Frandsen}$, values between 4 and 6 were noted to be the most common diffuseness levels to be encountered in natural scenes, such as in open scenes with both the sun and clouds in the sky. Translating these values into normalised values results in a range between 0.2 and 0.3, indicating much more directed light than the natural or preferred diffuseness levels mentioned above. Possible reasons for his misestimate might be that Frandsen did not test his statement by experiments and, moreover, neglected half the diffuseness range in his theory.

Although the perception of light diffuseness is based on the appearance of light sources and illuminated objects, neither the vector/scalar illumination ratio nor the first/zeroth order strength of the SH representation, strictly, are an index of object appearance. That is because the formation of the lighting pattern on an object is not only determined by the light diffuseness, but also by the light direction and light density, as well as by the geometric and scattering properties of surfaces and the viewing direction. That is why light diffuseness is different from a 'modelling index'. 'Modelling indices' depend on the light diffuseness, but do not represent the light diffuseness. Instead they (should) represent how well the lighting conditions make it possible to see 3D shapes in it. Light direction, light density, and other environmental characteristics together with diffuseness determine the appearance of objects, and so the modelling aspect.

The light diffuseness metrics $D_{Cuttle}$ and $D_{Xia}$ describe the relationship between the

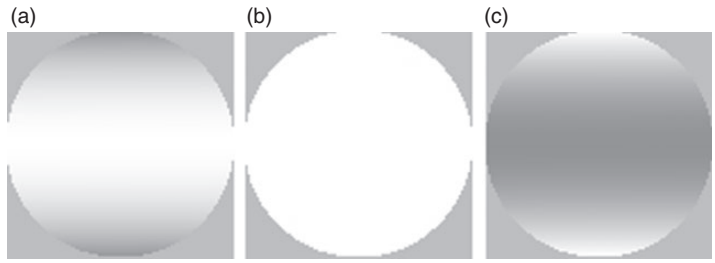


**Figure 8.** Light patterns on a Lambertian sphere with the light vector being zero: (a) a light ring; (b) uniform light field; (c) two opposed point light sources.

zeroth order and the first order SH components. Due to effects of second order SH contributions, identical values of $D_{Cuttle}$ or $D_{Xia}$ may result in different lighting patterns on an object. The second order SH component was called 'squash tensor' by Mury *et al.*,[19,47,48] because of its shape in extreme cases: a light or dark squash. For instance in Figure 8, the sphere is illuminated by a light ring (or dark squash) in Figure 8(a), a uniform light field in Figure 8(b) and two opposed light sources (or light squash) in Figure 8(c). In all three conditions, both the normalised $D_{Cuttle}$ and $D_{Xia}$ have a value of 1 (since the light vector is 0), but the illumination pattern on the sphere is different. Furthermore, adding an ambient term (zeroth order SH term) to the model 'probe in a sphere' simply contributes an additional uniform illumination over the surface of the spherical probe but would not influence the higher order SH components (e.g. the first order). Thus, such a change will result in a higher value of the normalised diffuseness.

Morgenstern *et al.* proved that the ICE is the ratio between the energy in the first to infinite orders and the energy in the zeroth order components of the SH representation of the illumination over a Lambertian sphere. Similar to the effect above, identical values of the ICE may result in different lighting patterns on an object. For example, varying the phase of the SH or shifting energy between harmonics within a single order has no effect on the ICE value, but does change the illumination pattern on an object. A well-known effect in this area concerns variations of the light vector direction with respect to a viewer, which changes the apparent diffuseness[18,27] but not the physical diffuseness. In future research, we will investigate how to capture such higher order angular variations (so-called light texture[32]) in descriptions, measurements and visualisations.

## 8. Conclusion

In this study, four well-known diffuseness metrics were reviewed and their relationships were examined via a model named 'probe in a sphere'. We proposed a light diffuseness metric $D_{Xia}$, which is entirely based on a mathematical description of the physical light distribution in a 3D space (the light field) and fulfils the criteria we defined for diffuseness metrics. Together with the light density and direction it forms a global integral description of the low order properties of the light field structure. It also allows easy extensions to descriptions of the high order components of the light field. Furthermore, the SH representation based method has the advantage that it is clear how the parameters relate and which role they play in the resulting light field. These properties and their variation in 3D space reflect the spatial and form-giving character of light.

## Declaration of conflicting interests

The author(s) declared no potential conflicts of interest with respect to the research, authorship, and/or publication of this article.

## Funding

The author(s) received no financial support for the research, authorship, and/or publication of this article.

## References

1 Raynham P. *The SLL Code for Lighting*. UK: The Society of Light and Lighting, 2012.
2 Hunter F, Biver S, Fuqua P. *Light – Science and Magic: An Introduction to Photographic Lighting*. London: Taylor and Francis, 2007.
3 Gurney J. *Color and Light: A Guide for the Realist Painter*. Riverside, NJ: Andrews McMeel Publishing, 2010.
4 Baxandall M. *Shadows and Enlightenment*. New Haven, CT: Yale University Press, 1997.
5 Ganslandt R, Hofmann H.. *Handbook of Lighting Design*. Ludenscheid, Germany: ERCO. 1992.
6 Cuttle C. *Lighting by Design*. Oxford: Architectural Press: Routledge, 2003:214.
7 Michel L. *Light: The Shape of Space: Designing with Space and Light*. Hoboken, NJ: John Wiley and Sons, 1995.
8 Kelly R. Lighting as an integral part of architecture. *College Art Journal* 1952; 12: 24–30.
9 Kelly R, Neumann D, Addington DM. *The Structure of Light: Richard Kelly and the Illumination of Modern Architecture*. New Haven, CT: Yale University Press, 2010.
10 Cuttle C. A new direction for general lighting practice. *Lighting Research and Technology* 2013; 45: 22–39.
11 Boyce P. *Lighting quality for all: Proceedings of SLL and CIBSE Ireland International Lighting Conference*, Dublin, Ireland, 12 April, 2013.
12 Kelly K, Duff J. Lighting design in Europe: Aligning the demands for lower energy usage with better quality. *Journal of Civil Engineering and Architecture* 2015; 9: 283–290.
13 Cuttle C. *Perceived adequacy of illumination: A new basis for lighting practice. Proceedings of the 3rd Professional Lighting Design Convention, Professional Lighting Designers Association*, Madrid, Spain, October 19–22: 2011: 27–31.
14 Koenderink JJ, Pont SC, van Doorn AJ, Kappers AML, Todd JT. The visual light field. *Perception* 2007; 36: 1595–1610.
15 Schirillo JA. We infer light in space. *Psychonomic Bulletin and Review* 2013; 20: 905–915.
16 Koenderink JJ, van Doorn AJ, Kappers AML, Pont SC, Todd JT. The perception of light fields in empty space. *Journal of Vision* 2005; 5: 558.
17 Te Pas SF, Pont SC. *A comparison of material and illumination discrimination performance for real rough, real smooth and computer generated smooth spheres*: *Proceedings of the 2nd Symposium on Applied Perception in Graphics and Visualization*, Spain: ACM, August 26–28: 2005: 75–81.
18 Pont SC, Koenderink JJ. Matching illumination of solid objects. *Perception and Psychophysics* 2007; 69: 459–468.
19 Mury AA, Pont SC, Koenderink JJ. Light field constancy within natural scenes. *Applied Optics* 2007; 46: 7308–7316.
20 Hallinan PW. *A low-dimensional representation of human faces for arbitrary lighting conditions*: *Proceedings of the IEEE Computer Society Conference on Computer Vision and Pattern Recognition*, *1994*, Seattle, WA: IEEE, June 21–22: 1994: 995–999.
21 Epstein R, Hallinan PW, Yuille AL. *5|spl plusmn|2 eigenimages suffice: an empirical investigation of low-dimensional lighting models*: *Proceedings of the IEEE Workshop on Physics-Based Modeling in Computer Vision, 1995*, Cambridge, MA, USA, June 18–19: 1995: 108–112.
22 Basri R, Jacobs DW. Lambertian reflectance and linear subspaces. *IEEE Transactions on Pattern Analysis and Machine Intelligence* 2003; 25: 218–233.
23 Ramamoorthi R, Hanrahan P. On the relationship between radiance and irradiance: Determining the illumination from images of a

convex Lambertian object. *Journal of the Optical Society of America A* 2001; 18: 2448–2459.
24 Gershun A. The light field (translated by Moon, PH and Timoshenko, G). *Journal of Mathematics and Physics* 1939; 18: 51–151.
25 Mury AA. *The light field in natural scenes*. Delft: Faculty of Industrial Design Engineering, Delft University of Technology, 2009.
26 Hewitt H, Bridgers D, Simons R. Lighting and the environment: Some studies in appraisal and design. *Lighting Research and Technology* 1965; 30: 91–116.
27 Cuttle C. Lighting patterns and the flow of light. *Lighting Research and Technology* 1971; 3: 171–189.
28 Lynes J, Burt W, Jackson G, Cuttle C. The flow of light into buildings. *Transactions of the Illuminating Engineering Society (London)* 1966; 31: 65–91.
29 Bean A. Modelling indicators for combined side and overhead lighting systems. *Lighting Research and Technology* 1978; 10: 199–202.
30 Waldram J. Studies in interior lighting. *Lighting Research and Technology* 1954; 19: 95–133.
31 Morgenstern Y, Geisler WS, Murray RF. Human vision is attuned to the diffuseness of natural light. *Journal of Vision* 2014; 14: 1–18.
32 Pont SC. Spatial and form-giving qualities of light. *Handbook of Experimental Phenomenology: Visual Perception of Shape, Space and Appearance*. Hoboken, NJ: John Wiley and Sons, 2013: pp. 205–222.
33 Frandsen S. *The scale of light – A new concept and its application*: *Proceedings of the 2nd European Conference on Architecture*, Paris, December 4–9: 1989: 4–8.
34 Morgenstern Y, Geisler WS, Murray RF. *The role of natural lighting diffuseness in human visual perception: Proceedings of IS&T/SPIE Electronic Imaging*. San Francisco, CA: International Society for Optics and Photonics, March 17 2015: 93940P–93940P.
35 Inanici M. *Computational approach for determining the directionality of light:directional-to-diffuseness ratio*: *Proceedings of Building Simulation*. Beijing, China, 3–6 September 2007: 1182–1188.
36 Aydın-Yağmur Ş, Dokuzer-Öztürk L. Determination of the harshness–softness attribute of shadows. *Lighting Research and Technology* 2015; 47: 993–1009.
37 Xia L, Pont SC, Heynderickx I. The visual light field in real scenes. *i-Perception* 2014; 5: 613–629.
38 Xia L, Pont SC, Heynderickx I. *The sensitivity of observers to light field in real scenes*: *Proceedings of Experiencing Light 2014, International Conference on the Effects of Light on Wellbing*, Eindhoven, the Netherlands, Nov 10–11: 2014: 120.
39 Kartashova T, de Ridder H, te Pas SF, Schoemaker M, Pont SC. *The visual light field in paintings of Museum Prinsenhof: Comparing settings in empty space and on objects: Proceedings of IS&T/SPIE Electronic Imaging*. San Francisco, CA: International Society for Optics and Photonics, March 9–10: 2015: 93941M–93941M.
40 Madsen M, Donn M. *Experiments with a digital "light-flow-meter" in daylight art museum buildings*: *5th International Radiance Scientific Workshop*, Leicester, UK, Sep 13–14: 2006.
41 Nassar A, El-Ganainy M, Moktader F, El-Kareem S, Haridi M. Cylindrical illuminance and its importance in integrating daylight with artificial light. *Lighting Research and Technology* 2003; 35: 217–222.
42 Duff JT, Kelly K. *In-field measurement of cylindrical illuminance and the impact of room surface reflectances on the visual environment*: *Proceedings of the SLL and CIBSE Ireland International Lighting Conference*, Dublin, Ireland, 12 April 2013: 1–11.
43 Rowlands E, Loe D. *Preferred illuminance distribution in interiors*: *Proceedings of 18th CIE Session, London*, 18–25 September 1975, P-75-17.
44 Cuttle C, Valentine W, Lynes J, Burt W. *Beyond the working plane*: *Proceedings of the CIE, Washington, DC*, 19–28 June 1967, P-67-12.
45 Cuttle C. Cubic illumination. *Lighting Research and Technology* 1997; 29: 1–14.
46 Cuttle C. Research Note: A practical approach to cubic illuminance measurement. *Lighting Research and Technology* 2014; 46: 31–34.

47 Mury AA, Pont SC, Koenderink JJ. The structure of light fields in natural scenes. *Applied Optics* 2009; 48: 5386–5395.
48 Mury AA, Pont SC, Koenderink JJ. Representing the light field in finite three-dimensional spaces from sparse discrete samples. *Applied Optics* 2009; 48: 450–457.
49 Stock RD, Siegel MW. Orientation invariant light source parameters. *Optical Engineering* 1996; 35: 2651–2660.